Numerical Simulations
of the Thread Rolling Process as Ecological
and Economical Research Tool
in the Implementation of Modern Technologies

Krzysztof Kukiełka
Politechnika Koszalińska

1. Introduction

In the twenty-first century, preparing the production of new products should be subject to "eco-design of the product," which consists to reduce the negative impact on the surrounding natural environment of man. The dominant role in this action plays the rational use of energy and environmental protection. In this aspect, it is important to develop a correct and proper implementation of technological process.

Volume plastic work on cold allows to achieve high accuracy of the product and high productivity in process like: thread rolling (Kukiełka K. 2009, Kukiełka K. & Kukielka L. 2013, Kukiełka K. 2014, Kukiełka K. et. al 2014, Kukiełka K. 2016, Kukiełka L. & Kukiełka K. 2007, Kukiełka L. & Kukiełka K. 2012), duplex burnishing (Patyk & Kukielka L. 2008, Patyk et al 2014), burnishing rolling (Kukiełka L. 1994, Kukiełka L. 1999, Kukiełka L. & Krzyżyński T. 2000, Kukiełka L. 2001, Kukiełka L. 2002, Kukiełka L. et al 2012, Kukiełka L. et al 2012, Kułakowska et al 2009, Kułakowska, Kukiełka L et al 2014, Myśliński et al 2004), drawpiece forming process (Kałduński & Kukielka L. 2014), shot penning (Zaleski & Bławucki 2014), grinding process (Sutowski & Nadolny 2016, Nadolny et al 2014), plastic deformations of measured object surface (Kowalik et al. 2016), surface roughness measured after machining (Valicek et al 2012, Kusnerova et al 2013), other like water jet

cutting (Perec 2016) and mechanical/abrasive polishing (MP), standard electropolishing (EP) and magnetoelectropolishing (MEP) (Rokosz 2016), plasma cutting (Skoczylas & Zaleski 2015) and modern material behaviour modelling (Malag et al 2014). The performance of machine parts using this technology, the use of the starting material is on average 85-97%, and material savings entail large energy savings. Savings should also include lower costs of storage material, the elimination of chips management, less need for cooling, lower expenditures on transport and depreciation of production equipment (Jednovicky & Streit 1998).

One of the post-machining methods employed to shape the outer layer, characterized by advantageous exploitation properties, is thread rolling. The thread rolling technology has many advantages, namely: saving material, extremely short times of execution, which affects on high performance of production, high durability of tools, make full use of existing machine park. In contrast to thread machining, after which the waste remains in the shape of chips, using a rolling technology as volume of the plastic working, it is possible to perform thread with total consumption of material. Diameter of the blank (bar or pipe) to the rolled thread is smaller than the diameter of the machined thread, and this results significant savings of material (Domblesky & Feng 2002, Kukiełka K. 2009, Kukiełka K. & Kukielka L. 2013, Kukiełka K. 2014, Kukiełka K. et al. 2014, Kukiełka K. 2016, Kukiełka L.& Kukiełka K. 2007, Kukiełka L. & Kukiełka K. 2012, Łyczko 2010, Olszak 2008).

Favourable strength (both static and dynamic) and exploitational properties of the rolled threads are the result of plastic deformation in the top layer of the part. In these threads, the material in the external layers is laid in the form of fibers covering the whole thread profile (Fig. 1), whereas in the threads made by cutting the fibers are cross-cut.

The heating of parts is realised whilst rolling, by means of visco-plastic deformation and fretting in the areas of contact between the roller and the objet (Fig. 2) (Kukielka L. 1994, Kukielka L. 1999, Kukielka, L. & Krzyzynski 2000, Kukielka L. et al. 2012, Kukielka L. et al., Kukiełka L. & Kukiełka K. 2015, Kukiełka K. 2017).
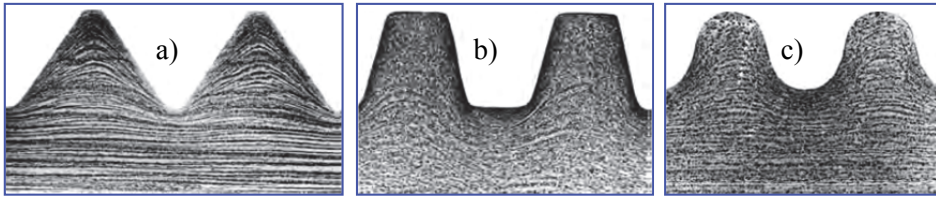
Fig. 1. Microstructure and texture of the rolled thread (St3 steel) a) M25 thread, b) trapezoidal thread, c) Round thread (Fette 2007)
Rys. 1. Mikrostruktura i tekstura gwintu wygniatanego (stal St3) a) gwint M25, b) gwint trapezowy, c) gwint okrągły (Fet2007)

Thread rolling is carried out with using a concentrated heat source, move together with the tool. These sources depending on their location are dived into plane and spatial sources. Plane sources appear in the contact zone of active surface of the roll with workpieces, while the spatial source occur inside the wok pieces and tools (Fig. 2).
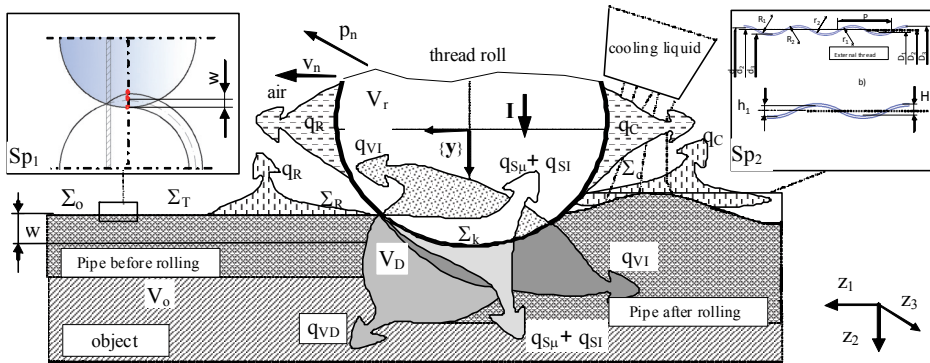

Fig. 2. Diagram of the system of heat fluxes arising in characteristic volumes V and areas $\sum$ during thread rolling: pipe before rolling and pipe after - surface of the object and outer layer after previous treatment and after rolling, respectively
Rys. 2. Schemat procesu z układem strumieni cieplnych powstających podczas obróbki, w charakterystycznych objętościach V i obszarach $\sum$ obiektu: Sp_1 i Sp_2 - rura odpowiednio po obróbce poprzedzającej i po walcowaniu

Energy of plane sources is the mechanical energy (friction roll-work pieces). During the friction heat is produced $q_{S\mu}$. Spatial sources of energy is the mechanical energy (plastic deformation of the material). During plastic deformation the heat q_{VD}. The total power of heat sources

is the sum of the mechanical power sources $q_{S\mu} + q_{VD}$, and wherein the value of the temperature distribution during the rolling process depends on the quotas for of those power sources. During the rolling, there are four variation stages of heat field, namely: the increase, almost stabilization, alignment, and decrease. Increase of the heat field it takes a place in the initial phase of rolling, upon commencement of operation of sources. The decrease of the heat field occurs in the final stage, once resolved these sources. For practical purposes it can be assumed that the temperature field is quasi-stationary, because instability the time periods are short and cooling conditions are selected as to achieve stable temperature field. Then, in any position of the tool, the temperature distribution is characterized by the presence of elongated isotherm (Fig. 3).
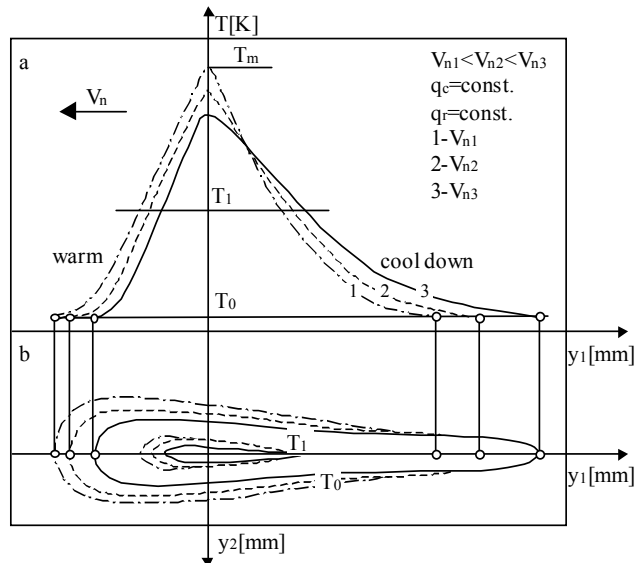

Fig. 3. Thermal cycle in massive body occurring during thread rolling at different speeds V_n and the constant cooling rate: a) the temperature distribution in the surface layer of the object in the direction of the velocity vector of the thread rolling b) isotherms T_0 and T_1
Rys. 3. Cykl cieplny w ciele masywnym zachodzący podczas walcowania z różnymi prędkościami V_n i stałej szybkości chłodzenia: a) rozkład temperatury w warstwie wierzchniej przedmiotu na kierunku wektora prędkości walcowania, b) rozkład izoterm T_0 i T_1.

The increase of the rolling speed at constant power of the heat sources and constant cooling rate causes elongated isotherm along y_1 axis (Fig. 3a) (on the direction of the rolling speed), while ahead of the source of the thermal field decreases. Followed by also narrowing of the isotherms perpendicular direction (Fig. 3b).

In the article (Kukielka K. 2017) shows the problem of modelling the thread rolling process with applying of advanced methods, which directly contributes to reduce the negative impact of this process on the surrounding environment. Ways to solve the received discrete equations of motion of the object together with an analysis and numerical simulation are presented in the work (Kukielka K. 2017).

In the this paper the solutions of discrete equations of the heat transfer of the object in the thread rolling process with applied explicit and implicit integrations methods, were shown. Described results of experimental investigations, which verify computational results and correctness of calculating model.

2. Algorithm of numerical analysis

In the paper (Kukielka K. 2017) the discretized equations of heat transfer equilibrium was obtained:

$$[^t\mathbf{C}]\{^\tau_t\Delta\dot{\boldsymbol{\Theta}}\} + ([^t\mathbf{K}^k] + [^t\mathbf{K}^c] + [^t\mathbf{K}^r] + [^t\mathbf{K}^{IV}])\{^\tau_t\Delta\boldsymbol{\Theta}\} = \{^\tau_t\Delta\mathbf{Q}\} + \{^\tau_t\Delta\mathbf{Q}^I\}, \quad (1)$$

where $[^t\mathbf{C}]$ and $[^t\mathbf{K}^k]$, $[^t\mathbf{K}^c]$, $[^t\mathbf{K}^r]$, $[^t\mathbf{K}^{IV}]$ are the convection and radiation, heat capacities, conductivity matrices and total nodal point conditions of IV gender, respectively:

$$[^t\mathbf{C}] = \sum_e^E \int_{t_{V^{(e)}}} {}^tc^{(e)\,t}\rho^{(e)}[^t\mathbf{H}^{(e)}]^T[^t\mathbf{H}^{(e)}]\,d^tV^{(e)},$$

$$[^t\mathbf{K}^k] = \sum_e^E \int_{t_{V^{(e)}}} [^t\mathbf{B}^{(e)}]^T[^t\lambda^{(e)}][^t\mathbf{B}^{(e)}]\,d^tV^{(e)},$$

$$[^t\mathbf{K}^c] = \sum_{m=1}^{S_C} \int_{t_{\Sigma_C^{(m)}}} {}^t\alpha_C[^t\mathbf{H}^{S(m)}]^T[^t\mathbf{H}^{S(m)}]\,d^t\Sigma_C^{(m)}), \quad (2)$$

$$[^t\mathbf{K}^r] = \sum_{m=1}^{S_R} \int_{t_{\Sigma_R^{(m)}}} {}^t\alpha_R[^t\mathbf{H}^{S(m)}]^T[^t\mathbf{H}^{S(m)}]\,d^t\Sigma_R^{(m)}),$$

$$[^t\mathbf{K}^{IV}] = \sum_{m=1}^{S_k} \left(\int_{t_{\Sigma_k^{(m)}}} \frac{[^t\mathbf{H}^{S(m)}]^T[^t\mathbf{H}^{S(m)}]}{{}^tR_s^{(m)}}\,d^t\Sigma_k^{(m)}\right)$$

E is the total number of the finite elements in the system, S_R, S_C, S_k are the number of the finite elements in the zones Σ_R, Σ_C and Σ_k, respectively.

The nodal point increment heat flow input vector $\{{}_t^\tau \Delta \mathbf{Q}\}$ is given by:

$$\{{}_t^\tau \Delta \mathbf{Q}\} = \{{}_t^\tau \Delta \mathbf{Q}_{VD}\} + \{{}_t^\tau \Delta \mathbf{Q}_{S\mu}\}, \qquad (3)$$

where:

$$\{{}_t^\tau \Delta \mathbf{Q}_{VD}\} = \sum_{e=1}^{E} \left(\int_{{}^t V_R^{(e)}} [{}^t \mathbf{H}^{(e)}]^T {}_t^\tau \Delta q_{VD}^{(e)} \, d^t V^{(e)} \right), \qquad (4)$$

$$\{{}_t^\tau \Delta \mathbf{Q}_{S\mu}\} = \sum_{m=1}^{S_k} \left(\int_{{}^t \Sigma_k^{(m)}} [{}^t \mathbf{H}^{S(m)}]^T {}_t^\tau \Delta q_{S\mu}^{(m)} [\cdot] \, d^t \Sigma_k^{(m)} \right).$$

The vector $\{{}_t^\tau \Delta \mathbf{Q}^I\} = \{{}_t^\tau \Delta \mathbf{Q}_S^I\} + \{{}_t^\tau \Delta \mathbf{Q}_V^I\}$ of the boundary conditions of I gender is given by:

$$\{{}_t^\tau \Delta \mathbf{Q}_S^I\} = \sum_{m=1}^{S_T} \left(\int_{{}^t \Sigma_T^{(m)}} [{}^t \mathbf{H}^{S(m)}]^T [{}^t \mathbf{H}^{S(m)}]_t^\tau \Delta \Theta_b^{(m)}\} \, d^t \Sigma_T^{(m)} \right),$$

$$\{{}_t^\tau \Delta \mathbf{Q}_V^I\} = \sum_{e=1}^{E_T} \left(\int_{{}^t \Sigma_k^{(m)}} [{}^t \mathbf{H}^{(e)}]^T [{}^t \mathbf{H}^{(e)}] \{{}_t^\tau \Delta \Theta_b^{(m)}\} \, d^t V_T^{(e)} \right),$$

$$\qquad (5)$$

where S_T and E_T are the number of the finite elements in the zones Σ_T and volume V_T, respectively.

Use the principles of step-by-step integration scheme (Kukielka L. & Kukielka K. 2015) in this section is presented for the solution of transient heat transfer problems. To approximate the velocity component $\{{}_t^\tau \Delta \dot{\Theta}\}$ in term of $\{{}_t^\tau \Delta \Theta\}$ in the equation (1) we can use the Euler method (with the temperature varies linearly over the time interval Δt) and the direct integration methods: the Houbolt method, the Wilson Θ method, and the Newmark method. In this paper, an example to using the Houbolt method to solution the equation (1) is showed. The Houbolt method reduces directly to a static analysis. The following finite approximate of the velocity component $\{{}_t^\tau \Delta \dot{\Theta}\}$ is employed:

$$\{{}_t^\tau \Delta \dot{\Theta}\} = a_1 \{{}_t^\tau \Delta \Theta\} - a_2 \{{}^t \Theta\} + a_3 \{{}^{t-\Delta t} \Theta\} - a_4 \{{}^{t-2\Delta t} \Theta\}, \qquad (6)$$

where:

$$a_1 = 11/(6\Delta t), \ a_2 = 7/(6\Delta t), \ a_3 = 3/(2\Delta t), \ a_4 = 1/(3\Delta t), \qquad (7)$$

are the integral constants.

Substituting (6) into (1) and arranging all known vectors on the right-hand side, we obtain for the solution of $\{_t^\tau \Delta\boldsymbol{\Theta}\}$:

$$[^t\widetilde{\mathbf{K}}]\{_t^\tau\Delta\boldsymbol{\Theta}\} = \{_t^\tau\Delta\widetilde{\mathbf{Q}}\} + \{^t\widetilde{\mathbf{Q}}\}, \tag{8}$$

where:

$$[^t\widetilde{\mathbf{K}}] = a_1[^t\mathbf{C}] + [^t\mathbf{K}^k] + [^t\mathbf{K}^c] + [^t\mathbf{K}^r] + [^t\mathbf{K}^{IV}], \tag{9}$$

$$\{^t\widetilde{\mathbf{Q}}\} = [^t\mathbf{C}](a_2\{^t\boldsymbol{\Theta}\} - a_3\{^{t-\Delta t}\boldsymbol{\Theta}\} + a_4\{^{t-2\Delta t}\boldsymbol{\Theta}\}), \tag{10}$$

$$\{_t^\tau\Delta\widetilde{\mathbf{Q}}\} = \{_t^\tau\Delta\mathbf{Q}\} + \{_t^\tau\Delta\mathbf{Q}^I\}. \tag{11}$$

As shown in (10) the solution of $\{_t^\tau\Delta\boldsymbol{\Theta}\}$ required knowledge of $\{^t\boldsymbol{\Theta}\}$, $\{^{t-\Delta t}\boldsymbol{\Theta}\}$ and $\{^{t-2\Delta t}\boldsymbol{\Theta}\}$. Although the knowledge of $\{^0\Delta\boldsymbol{\Theta}\}$ and $\{^0\Delta\dot{\boldsymbol{\Theta}}\}$ is useful to start the Houbolt integration scheme, it is more accurate to calculate $\{^{\Delta t}\boldsymbol{\Theta}\}$ and $\{^{2\Delta t}\boldsymbol{\Theta}\}$ by some other means; i.e., we employ special starting procedures. One way of the proceeding is to integrate (1) for the solution of $\{^{\Delta t}\boldsymbol{\Theta}\}$ and $\{^{2\Delta t}\boldsymbol{\Theta}\}$ using a different integration scheme, possibly a conditionally stable method such as the central difference scheme such as the central difference scheme with a fraction of Δt as the time step. The complete algorithm used in the integration is given in Table 1.

Table 1. Step-By-Step Solution Using Houbolt Integration Method
Tabela 1. Rozwiązanie Krok po Kroku przy wykorzystaniu metody całkowania Houbolt

---

A. *Initial Calculations:*

  1. Form matrix $[^t\mathbf{C}], [^t\mathbf{K}^k], [^t\mathbf{K}^c], [^t\mathbf{K}^r]$ and $[^t\mathbf{K}^{IV}]$.

  2. Initialise $\{^0\boldsymbol{\Theta}\}$ and $\{^0\dot{\boldsymbol{\Theta}}\}$.

  3. Select time step Δt and calculate integration constants:
    $a_1 = 11/(6\Delta t),\ a_2 = 7/(6\Delta t),\ a_3 = 3/(2\Delta t),\ a_4 = 1/(3\Delta t).$

  4. Use special starting procedure to calculate $\{^{\Delta t}\boldsymbol{\Theta}\}$ and $\{^{2\Delta t}\boldsymbol{\Theta}\}$.

  5. Calculate effective matrix $[^t\widetilde{\mathbf{K}}]$:

$$[^t\widetilde{\mathbf{K}}] = a_1[^t\mathbf{C}] + [^t\mathbf{K}^k] + [^t\mathbf{K}^c] + [^t\mathbf{K}^r] + [^t\mathbf{K}^{IV}].$$

B. *For Each Time Step*

1. Calculate effective heat load at time t:

$$\{^{t}\widetilde{\mathbf{Q}}\} = [^{t}\mathbf{C}](a_2\{^{t}\mathbf{\Theta}\} - a_3\{^{t-\Delta t}\mathbf{\Theta}\} + a_4\{^{t-2\Delta t}\mathbf{\Theta}\}).$$

2. Calculate effective incremental heat load at time step t→τ:

$$\{^{\tau}_{t}\Delta\widetilde{\mathbf{Q}}\} = \{^{\tau}_{t}\Delta\mathbf{Q}\} + \{^{\tau}_{t}\Delta\mathbf{Q}^{I}\}.$$

3. Partition of the heat equilibrium equation for two blocks, we can write the problem in the form:

$$\begin{bmatrix} [^{t}\widetilde{\mathbf{K}}_{11}^{nxn}] & [^{t}\widetilde{\mathbf{K}}_{12}^{nxw}] \\ [^{t}\widetilde{\mathbf{K}}_{21}^{wxn}] & [^{t}\widetilde{\mathbf{K}}_{22}^{wxw}] \end{bmatrix} \begin{Bmatrix} \{^{\tau}_{t}\Delta\mathbf{\Theta}_{1}^{nx1}\} \\ \{^{\tau}_{t}\Delta\mathbf{\Theta}_{2}^{wx1}\} \end{Bmatrix} = \begin{Bmatrix} \{^{\tau}_{t}\Delta\widetilde{\mathbf{Q}}_{1}^{nx1}\} \\ \{^{\tau}_{t}\Delta\widetilde{\mathbf{Q}}_{2}^{wx1}\} \end{Bmatrix} + \begin{Bmatrix} \{^{t}\widetilde{\mathbf{Q}}_{1}^{nx1}\} \\ \{^{t}\widetilde{\mathbf{Q}}_{2}^{wx1}\} \end{Bmatrix},$$

where vectors $\{^{\tau}_{t}\Delta\mathbf{\Theta}_{2}^{wx1}\}$, $\{^{\tau}_{t}\Delta\widetilde{\mathbf{Q}}_{1}^{nx1}\}$ are knows and $\{^{\tau}_{t}\Delta\mathbf{\Theta}_{1}^{nx1}\}$, $\{^{\tau}_{t}\Delta\widetilde{\mathbf{Q}}_{2}^{wx1}\}$ are not known.

4. Solve for temperature increment vector $\{^{\tau}_{t}\Delta\mathbf{\Theta}_{2}^{wx1}\}$ at time step using the modified Newton-Raphson iteration method:

$$[^{t}\widetilde{\mathbf{K}}_{11}]_{nxn}^{[i-1]}\{^{\tau}_{t}\Delta\mathbf{\Theta}_{1}\}_{nx1}^{[i]} = \{^{\tau}_{t}\Delta\widetilde{\mathbf{Q}}_{1}\}_{nx1}^{[i-1]} + \{^{t}\widetilde{\mathbf{Q}}_{1}\}_{nx1} - [^{t}\widetilde{\mathbf{K}}_{12}]_{nxw}^{[i-1]}\{^{\tau}_{t}\Delta\mathbf{\Theta}_{2}\}_{wx1}.$$

5. Substituting vector $\{^{\tau}_{t}\Delta\mathbf{\Theta}_{1}^{nx1}\}$ into equation:

$$\{^{t}\widetilde{\mathbf{Q}}_{2}\}_{wx1}^{[i]} = [^{t}\widetilde{\mathbf{K}}_{21}]_{wxn}^{[i-1]}\{^{\tau}_{t}\Delta\mathbf{\Theta}_{1}\}_{nx1}^{[i]} + [^{t}\widetilde{\mathbf{K}}_{22}]_{wxw}^{[i-1]}\{^{\tau}_{t}\Delta\mathbf{\Theta}_{2}\}_{wx1} - \{^{t}\widetilde{\mathbf{Q}}_{2}\}_{wx1},$$

and solve we obtain the vector $\{^{\tau}_{t}\Delta\widetilde{\mathbf{Q}}_{2}\}_{wx1}^{[i]}$.

6. Calculate the temperature vector at the end of iteration i:

$$\{^{\tau}\mathbf{\Theta}\}^{[i]} = \{^{t}\mathbf{\Theta}\}^{[i-1]} + \{^{\tau}_{t}\Delta\mathbf{\Theta}\}^{[i]}.$$

7. Calculate vector $\{^{\tau}_{t}\Delta\dot{\mathbf{\Theta}}\}$ at step time:

$$\{^{\tau}_{t}\Delta\dot{\mathbf{\Theta}}\} = a_1\{^{\tau}_{t}\Delta\mathbf{\Theta}\} - a_2\{^{t}\mathbf{\Theta}\} + a_3\{^{t-\Delta t}\mathbf{\Theta}\} - a_4\{^{t-2\Delta t}\mathbf{\Theta}\}.$$

3. THREAD ROLLING application for numerical analysis

Developed by author application THREAD ROLLING in ANSYS system fully satisfy advanced requirements and can be successfully used to simulate thread rolling process in real conditions. In this application the algorithm shown in point 2 were applied. Increasing technical and economic requirements also decrease negative impact on environment lead to search for new technology and materials, which require the development of new theoretical models and their numerical implementation. This article presents the practical application called THREAD ROLLING to modeling and simulation process of thread rolling with round outline. The purpose of a computer simulation is to restore investigated process base on a mathematical model by using a computer and examine the impact of the environment (input signals) and internal properties of an object (process parameters) on the characteristics of the object.

The main advantages of computer simulation in comparison with other methods of the process analysis are:
− the model flexibility – is easy to making changes in the simulated model also filling model with new phenomena,
− easy to introduce various types of extortion and disturbance (random) and extreme extortion and disturbance without destroying usually expensive material model,
− relatively low cost and short preparation time of simulation,
− the reliability of simulation results - especially when we can compare the simulation results with the results obtained from measurements on a real object.

Numerical calculations in ANSYS system were realized by the following sequence:
a) data preparation (PREPROCESSOR):
− defining the workpieces and the tool geometry,
− defining the material properties of the workpiece and tool (depends of temperature),
− generating the finite element grid (mesh),
− defining contact between tool-workpieces, by introducing the contact finite element TARGET and CONTA,
− applying boundary condition (displacement, forces, temperatures),

b) solving (SOLVER)
− introducing number of steps and iterations, convergence conditions, etc.
− setting the course of calculations,
c) analysis of solutions and edit the results (POSTPROCESSOR - General Postproc or Time History Postproc).

4. Examples of numerical solution

Elaborated application THREAD ROLLING for spatial (3D) and plane (2D), with assumption of spatial state of stress and plane state of displacement and strain. In the exemplary simulation is shown the possibility of using reduced model to simulate the impact of the flat profile of the working rollers active surface on the thread rolling process realization and quality. The tool is a rigid body $E \to \infty$, however the model material as an elasto/thermo-visco-plastic body with nonlinear hardening (Fig. 4). The model has discretized by finite element PLANE184 with linear function of the shape. Shape coefficient (SC=B/A=1) rectangular finite element is define as a ratio height B to width A of elements (Fig. 4).
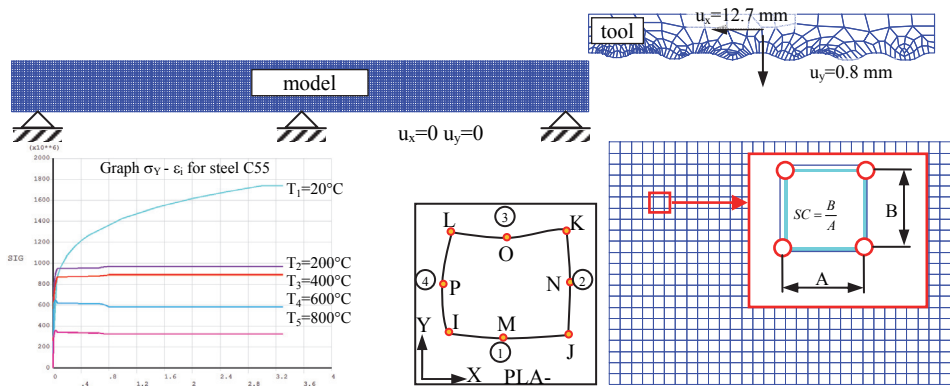

Fig. 4. Discretized computational model 2D for the external thread rolling with round profile
Rys. 4. Dyskretny model komputerowy 2D dla procesu walcowania gwintów zewnętrznych z okrągłym profilem

In the contact zone the boundary conditions for displacement are unknown. The calculation was carried out for following properties: rolling by means of a $D = 61$ mm diameter roller-shaped element; depth of rolling $w = 0.8$ mm; velocity of rolling $v_r = 0.025$, 0.05, 0.1 m·s^{-1}; object material – steel C55, roller – 145Cr6; heat conductivity coefficients $\lambda_{(o)} = 42 - 0.012 \cdot \Delta T$ W·m^{-1}·K^{-1}; $\lambda_{(r)} = 13.2207 \ -0.0032 \cdot \Delta T$ W·m^{-1}·K^{-1}; mass density $\rho = 7850/(1 + 3 \cdot \alpha \cdot \Delta T)$ g·m^{-3}; heat capacity $c = 484 + 0.01 \cdot \Delta T$ J·(kg·K)$^{-1}$; coefficient of fretting $\mu = \mu_0(1 - 0.003 \cdot v_r)(1 - 0.000015 \cdot \Delta T)$; heat resistance in the surface contact $R_s = 0$ (ideal contact) and $R_S = 0.094$ m^2·K·W^{-1} (real contact), yield stress ${}_t^t\sigma_Y = 924(0.066 + {}_t^t\varepsilon_i^{(VP)})^{0.18} \times (1 + {}_t^t\dot{\varepsilon}_i^{(VP)})^{0.15}(1.737 - 0.043 \, {}^t T^{1/2})$ MPa, where ${}_t^t\varepsilon_i^{(VP)}$ and ${}_t^t\dot{\varepsilon}_i^{(VP)}$ are intensity of true strain and strain rate at time t, respectively, Young's modulus $E = 5 \cdot 10^{11} \cdot T^{-0.259}$ GPa, Poisson's ratio $\nu = 0.299 \cdot T^{0.0193}$.

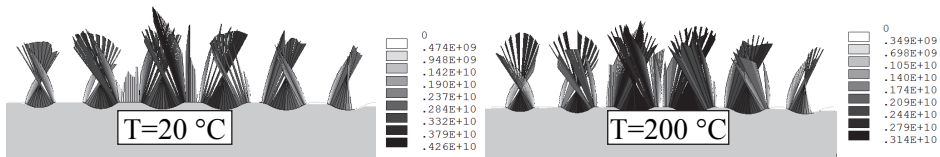The nonlinear analysis of the temperature in the contact zone is demonstrated in the Figure 5-7.

Fig. 5. Distribution of the contact pressure (MPa) for successive rings during the thread rolling process with round outline for various value of temperature
Rys. 5. Rozkład nacisków kontaktowych (MPa) dla kolejnych pierścieni rolki podczas procesu walcowania gwintów z okrągłym profilem dla różnych wartości temperatury

The results for contact pressure during the thread rolling process are shown on Fig. 5. We can observed that increase of the temperature of rolled materials decrease the value of contact pressure. The distribution of the displacement vector sum (1), m, maps of equivalent plastic total strain Huber-Mises-Hencky's (2), maps of equivalent total stress Huber-Mises-Hencky's, (3) after thread rolling process with round outline for temperature 20°C and 200°C we can observe respectively on Figs. 6 and

7. The value of displacement vector sum is still the same, but for strain and stress the value is smaller for higher temperature.
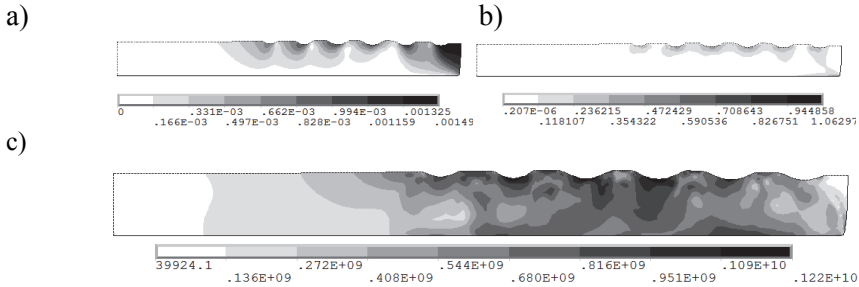
a)   b)

c)

Fig. 6. Distribution of the displacement vector sum, m (a), maps of equivalent plastic total strain Huber-Mises-Hencky's (b), maps of equivalent total stress Huber-Mises-Hencky's, MPa (c) after thread rolling process with round outline for temperature 20°C
Rys. 6. Rozkład wektora przemieszczeń wypadkowych, m (a), mapa całkowitych plastycznych odkształceń zastępczych według hipotezy Hubera-Mises'a-Hencky'ego (b), mapa całkowitych naprężeń zastępczych według hipotezy Hubera-Mises'a-Hencky'ego, MPa (c) po procesie walcowania gwintów okrągłych dla temperatury 20°C
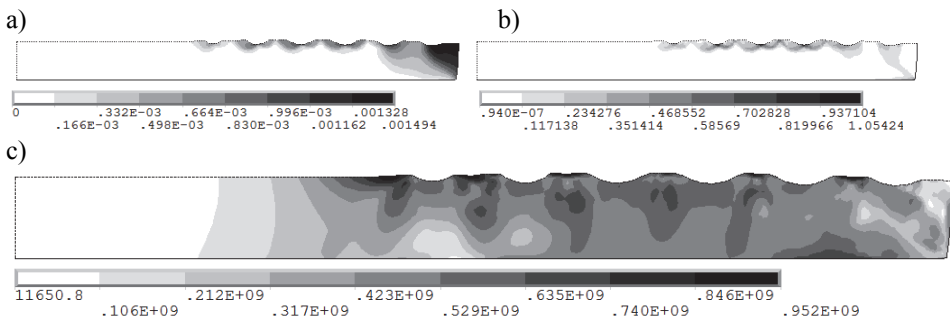
a)   b)

c)

Fig. 7. Distribution of the displacement vector sum (a), m, maps of equivalent plastic total strain Huber-Mises-Hencky's (b), maps of equivalent total stress Huber-Mises-Hencky's, MPa (b) after round thread rolling process for temperature 200°C
Rys. 7. Rozkład wektora przemieszczeń wypadkowych (a) m, mapa całkowitych plastycznych odkształceń zastępczych według hipotezy Hubera-Mises'a-Hencky'ego (b), mapa całkowitych naprężeń zastępczych według hipotezy Hubera-Mises'a-Hencky'ego, MPa (c) po procesie walcowania gwintów okrągłych dla temperatury 200°C

From the environmental point of view must be increased rolling speed, since it reduces the processing time. In the figure 8 it shows the effect of rolling speed on the temperature field in object and tool for ideal contact and for the occurrence of thermal resistance and coefficient of friction $\mu_0 = 0.2$.
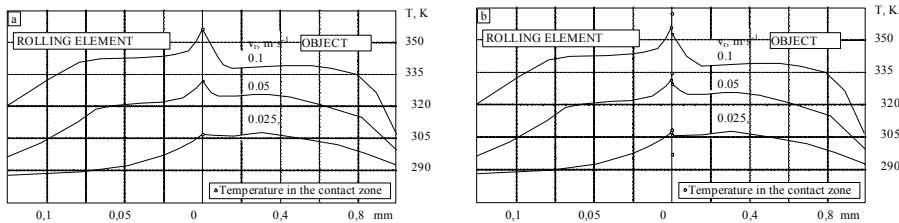

Fig. 8. Distribution of resultant temperature inside the roller and the object in axis z_2 for ideal contact (a) and with heat resistance in the surface contact (b)
Rys. 8. Rozkład wypadkowej temperatury wewnątrz rolki i na przedmiocie na osi z_2 dla idealnego kontaktu (a) oraz z opornością cieplną wewnątrz powierzchni kontaktu (b)

5. Experimental verification

Proposed in this paper a new way through the centerless rolling doesn't have the above drawbacks. The essence of this approach is to eliminate the fixed steady and the introduction of a system which contains four roller rolling surface (Fig. 9). The head is designed to conventional lathes and is fastened in place of the chuck. Head design allows for easy change of force and roller change (Kukiełka K. 2009, Kukiełka K. & Kukielka L. 2013, Kukiełka K. 2014, Kukiełka K. et al. 2014, Kukiełka K. 2016). In the working zone rolling fluid is given. The cyclic process of gradual loading, forming, calibrating and unloading is repeated until the desired length of thread is received. On the Fig 9. The real working head system during the thread rolling process is shown, where the temperature is measured by thermo visual hand camera made by Flir (Fig 9).

Figure 10 shows the temperature distributions during rolling of the pipes in the contact zone and outside it for different velocity rate, ie. $v = 0.025, 0.1$ m·s^{-1}. From conducted researches of measuring temperatures indicates the growth of rolling speed directly affects the growth of the temperature, the highest values is observed in the contact zone and after the roll-

ing process, that are the direct result of plastic deformation. For example, for a speed of $v = 0.025$ m·s^{-1} maximum measured temperature was 25.8°C, while the speed $v = 0.1$ m·s^{-1} reached value to 58.9°C.
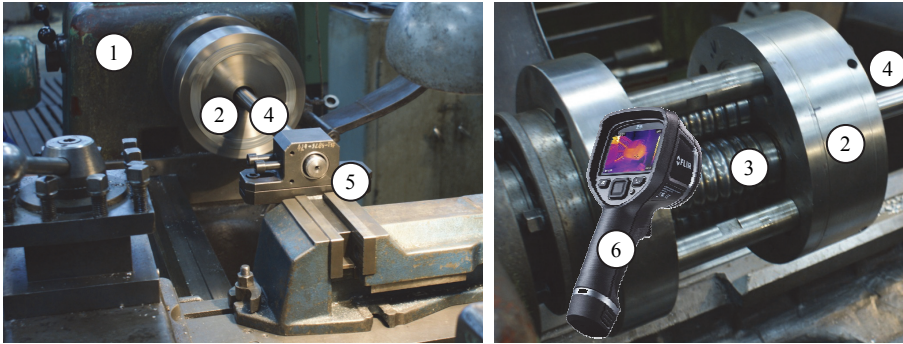

Fig. 9. Rolling system: 1 – conventional lathe, 2 – angular thread rolling head, 3 – rolling rolls, 4 – workpiece 5 – handle the workpieces in vice, 6 – manual thermal imaging camera Flir

Rys. 9. Układ obróbkowy: 1 – tokarka konwencjonalna, 2 – kątowa głowica do walcowania gwintów, 3– rolki walcujące, 4 – przedmiot obrabiany, 5 – uchwyt przedmiotu w imaku nożowym, 6 – ręczna kamera termowizyjna firmy Flir
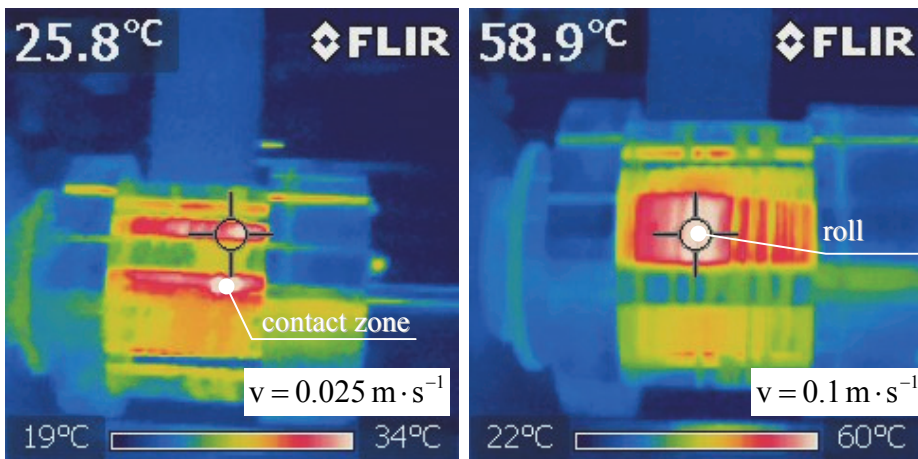

Fig. 10. The temperature distributions during rolling of the pipe for different velocity rate, ie. $v = 0.025, 0.1$ m·s^{-1}

Rys. 10. Rozkład temperatury podczas procesu walcowania rur dla różnych wartości prędkości, tj. $v = 0.025, 0.1$ m·s^{-1}

6. Conclusions

The presented method of numerical calculation of temperature fields is correct for any rolling conditions and the state of the output object and the history of his material. Using the application THREAD ROLLING it is possible to carry out a comprehensive analysis of thermal phenomena occurring during the thread rolling process. Can specify either the temperature distribution and the distribution of heat fluxes in the rolling zone for specified processing conditions, or conversely – for required temperature is possible to determined output state of the object and the conditions for implementation of rolling – include technological parameters (ie. velocity and depth of rolling).

The example shown illustrates how it affects the speed of rolling on temperature distribution, contact forces and the state of displacement, strain and stress in the object.

Application THREAD ROLLING in ANSYS system enables a complex time analysis of deformation (displacements, strains), forces, contact pressure, states of stresses and temperature occurring in object folding from a workpieces and a tool. It is possible to make a complete analysis for following data:

− any object geometry (eg. shaft, sleeve) and tools (an outline of the active surface, the number of rings, etc.)
− any material of workpieces and the tools material (Young's modulus, Poisson ratio, initial yield stress, tangent modulus, nonlinear dependence of the properties plastic materials: strain and strain rate, temperature and various models of hardening),
− different conditions of friction in the contact area,
− any horizontal and vertical movement of the tool in time.

The use of thread rolling process in place of the traditional methods of formulation through the loss of material gives a very large benefits in terms of environmental protection. Thread rolling process is carried out in about ten-fold less. In addition, the new processing technology is an innovation process and is a breakthrough character of technology because it replaces the machining method by plastic shaping threads. The use of traditional treatments produces waste in the form of chips sliced material,

dust, noise and waste coolant from machine tools – contaminated emulsion, which is hardly workable waste and require special disposal.

Additional benefits in terms of environmental protection resulting from the application of modern methods of production preparation, through the application of numerical simulation methods in place of the traditional long-term iterative process of reaching the required solution by experimental study.

References

Domblesk, J.P., Feng, F. (2002). Two-dimensional and three-dimensional finite element models of external thread rolling. *Professional Engineering Publishing*, *216(4)*, 507-517.

Jednovicky, B., Streit, J. (1998). *Cold volume treatment in market economy conditions*. Scientific-Technical Conference on Modern Cold Plastic Metalforming Technologies, Poznań- Kiekierz, 147-151. (in Polish).

Kaldunski, P., Kukielka, L., (2014). Numerical Analysis and Simulation of Drawpiece Forming Process by Finite Element Method, *Mechanics and Materials "Novel Trends in Production Devices and Systems", 474*, 153-158.

Kowalik, M., Rucki, M., Paszta, P., Gołębski, R. (2016). *Plastic deformations of measured object surface in contact with undeformable surface of measuring tool*. Measurement Science Review. *16(5)*, 254-259.

Kukiełka, K. (2009). *Modelling and numerical analysis of the states of deformations and stresses in the surface layer of the trapezoidal and round threads rolled on cold*. PhD Thesis, Koszalin University of Technology. (in Polish).

Kukiełka, K., Kukiełka, L. (2013). *External thread rolling head*. The polish patent No PL402652–A1, PL220175–B1, 4.02.2013. (in Polish).

Kukiełka, K. (2014). Effective numerical model to analyze the trapezoidal thread rolling process with finite element method. *Mechanik*, *11*, 156-167. (in Polish).

Kukielka, K., Kukielka, L., Bohdal, L., Kulakowska, A., Malag, L., Patyk, R. (2014). 3D Numerical Analysis the State of Elastic/Visco–Plastic Strain in the External Round Thread Rolled on Cold. *Applied Mechanics and Materials „Novel Trends in Production Devices and Systems", 474*, 436-441.

Kukielka, K. (2016). Ecological Aspects of the Implementation of New Technologies Processing for Machinery Parts. *Rocznik Ochrona Środowiska (Annual Set of Environment Protection)*, *18*, 137-157.

Kukiełka, K. (2017). Ecological and economical aspects of modern modeling of thread rolling process. *Rocznik Ochrona Środowiska (Annual Set of Environment Protection)*, *19*.

Kukiełka, L. (1994). *Theoretical and experimental foundations of surface roller burnishing with the electrocontact heating.* Book WM nr 47. WSI Koszalin. (in Polish)

Kukielka, L. (1999). Application of the variational and finite element methods to dynamic incremental nonlinear analysis in the burnishing rolling operation. *ESM'99 - Modelling And Simulation A Tool For The Next Millennium*, Vol. II, 221-225.

Kukielka, L., Krzyzynski T. (2000). New thermo-elastic thermo-visco-plastic material model and its application. *Zeitschrift Fur Angewandte Mathematik Und Mechanik*, Vol. 80, supplement: 3, S595-S596.

Kukielka, L. (2001). Mathematical modelling and numerical simulation of non-linear deformation of the asperity in the burnishing cold rolling operation. *Computational Methods in Contact Mechanics V, Book Series: Computational and Experimental Methods*, 5, 317-326.

Kukiełka, L. (2002). *Bases of engineering research*. PWN, Warsaw. (in Polish).

Kukielka, L., Kustra, J., Kukielka, K. (2005). Numerical analysis of states of strain and stress of material during machining with a single abrasive grain. *Computer Methods and Experimental Measurements for Surface Effects and Contact Mechanics VII*, Southampton–Boston, WIT*PRESS*, 57-66.

Kukielka, L., Kukielka, K. (2006). Numerical analysis of the process of trapezoidal thread rolling. *High Performance Structures and Materials III*,. Southampton–Boston, WIT*PRESS*, 663-672.

Kukielka, L., Kukielka, K. (2007). Numerical analysis of the physical phenomena in the working zone in the rolling process of the round thread. *Computer Methods and Experimental Measurements for Surface Effects and Contact Mechanics VIII*, Southampton–Boston, WIT*PRESS,* 125-124.

Kukiełka, L. (2010). New damping of models of metallic materials and its application in non–linear dynamical cold processes of metal forming. *The 13th International Conference Metal Forming 2010*, *Steel Research International*, Toyohashi, *81*, 1482-1485.

Kukielka, L., Geleta, K., Kukielka, K. (2012). Modelling and Analysis of Non-linear Physical Phenomena in the Burnishing Rolling Operation with Electrical Current. *Steel Research International, Special Edition: 14th International Conference Metal Forming*, Kraków, 1379-1382.

Kukielka, L., Geleta, K., Kukielka, K. (2012). Modelling of Initial and Boundary Problems with Geometrical and Physical Nonlinearity and its Application in Burnishing Processes. *Steel Research International, Special Edition: 14th International Conference Metal Forming*, Krakow, 1375-1378.

Kukiełka, L., Kukiełka, K. (2012). The modern method of modeling and analysis precision machining processes auto parts. *Environmental aspects of the use of new technologies in transport, Book of Mechanical Engineering*, No 235 of Mechanical Faculty, Koszalin University of Technology. Koszalin, 109-128 (in Polish)

Kukiełka, L., Bohdal, Ł., Chodór, J., Forysiewicz, M., Geleta, K., Kałduński P., Kukiełka, K., Patyk, R., Szyc, M. (2012). Numerical analysis of selected processes precision machining of automotive parts. *Environmental aspects of the use of new technologies in transport, Book of Mechanical Engineering No 235 of Mechanical Faculty*, Koszalin University of Technology, Koszalin, 129-194.

Kukielka, L., Kukielka, K., Kulakowska, A., Patyk, R., Malag, L., Bohdal, L. (2014). Incremental Modelling and Numerical Solution of the Contact Problem between Movable Elastic and Elastic/Visco–Plastic Bodies and Application in the Technological Processes. *Applied Mechanics and Materials "Novel Trends in Production Devices and Systems", 474*, 159-165.

Kukiełka, L., Kukiełka, K. (2015). Modelling and analysis of the technological processes using finite element method. *Mechanik, 88*, 317-340.

Kukielka, L., Szczesniak, M., Patyk, R., Kulakowska, A., Kukielka, K., Patyk S., Gotowala, K., Kozak, D. (2016). Analysis of the states of deformation and stress in the surface layer of the product after the burnishing cold rolling operation. *Novel Trends in Production Devices and Systems "Materials Science Forum"*.

Kulakowska, A., Patyk, R., Kukielka, L. (2009). Numerical analysis and experimental researches of burnishing rolling process of workpieces with real surface. *WMSCI 2009 – The 13th World Multi–Conference on Systemics, Cybernetics and Informatics, Jointly with the 15th International Conference on Information Systems Analysis and Synthesis, ISAS, 2*, 63-68.

Kulakowska, A., Kukielka, L., Kukielka, K., Malag, L., Patyk, R., Bohdal, L. (2014). Possibility of steering of product surface layers properties in burnishing rolling process. *Applied Mechanics and Materials "Novel Trends in Production Devices and Systems", 474*, 442-447.

Kusnerova, M., Valicek, J., Harnicarova, M., Hryniewicz, T., Rokosz, K., Palkova, Z., Vaclavik, V., Repka, M., Bendova, M. (2013). A Proposal for Simplifying the Method of Evaluation of Uncertainties in Measurement Results. *Measurement Science Review, 13(1)*, 1-6.

Łyczko, K. (2010). *External thread rolling technology*. WNT, Warszawa. (in polish).

Malag, L., Kukielka, L., Kukielka, K., Kulakowska, A., Patyk, R., Bohdal, L. (2014). Problems Determining of the Mechanical Properties of Metallic Materials from the Tensile Test in the Aspect of Numerical Calculations of the Technological Processes. *Applied Mechanics and Materials "Novel Trends in Production Devices and Systems", 474*, 454-459.

Nadolny, K., Plichta, J., Sutowski, P. (2014). Regeneration of grinding wheel active surface using high-pressure hydro-jet. *Journal Of Central South University, 21(8)*, 3107-3118.

Olszak, W. (2008). *Machining*. WNT, Warszawa. (in polish)

Patyk, R., Kukielka, L. (2008). Optimization of geometrical parameters of regular triangular asperities of surface put to smooth burnishing. *The 12th International Conference Metal Forming 2008, Steel Research International,* Kraków, *2*, 642-647.

Patyk, R. (2010). Theoretical and experimental basis of regular asperities about triangular outline embossing technology. *The 13th International Conference Metal Forming 2010, Steel Research International*, Toyohashi, *81*, 190-193.

Patyk, R., Kukielka, L., Kukielka, K., Kulakowska, A., Malag, L., Bohdal, L. (2014). Numerical Study of the Influence of Surface Regular Asperities Prepared in Previous Treatment by Embossing Process on the Object Surface Layer State after Burnishing. *Applied Mechanics and Materials "Novel Trends in Production Devices and Systems"*, *474*, 448-453.

Perec, A. (2016). *Abrasive suspension water jet cutting optimization using orthogonal array design*. International Conference on Manufacturing Engineering and Materials, ICMEM 2016,6-10 June 2016, Nový Smokovec. Procedia Engineering, *149*, 366-373.

Perec, A., Pude, F., Stirnimann, J., Wegener, K. (2015). *Feasibility study on the use of fractal analysis for evaluating the surface quality generated by waterjet*. Tehnički vjesnik, *22*, 4, 879-883.

Rokosz, K., Hryniewicz, T. (2016). *XPS Analysis of nanolayers obtained on AISI 316L SS after Magnetoelectropolishing*. World Scientific News, *37*, 232-248.

Skoczylas, A., Zaleski, K. (2015). Effect of Plasma Cutting Parameters upon Shapes of Bearing Curve of C45 Steel Surface. *Advances in Science and Technology Research Journal, 9(27)*, 78-82.

Staniszewski, B. (1980). *Heat transfer*. PWN, Warsaw.

Sutowski, P., Nadolny, K. (2016). The identification of abrasive grains in the decohesion process by acoustic emission signal patterns. *International Journal Of Advanced Manufacturing Technology*, *87(1-4)*, 437-450.

Valicek, J., Drzik, M., Hryniewicz, T., Harnicarova M., Rokosz K, Kusnerova M., Barcova K., Brazina D. (2012). Non-Contact Method for Surface Roughness Measurement After. Machining. *Measurement Science Review*, *12(5)*, 184-188.

Zaleski, K., Bławucki, S. (2015). Evaluation of the Effectiveness of the Shot Peening Process for Thin-Walled Parts Based on the Diameter of Impression Produced by the Impact of Shot Media. *Advances in Science and Technology Research Journal, 9(26)*, 77-82.

Symulacje numeryczne procesu walcowania gwintów jako ekologiczne i ekonomiczne narzędzie badawcze w procesie wdrażania nowoczesnych technologii

Streszczenie

W pracy przedstawiono sposób rozwiązywania dyskretnego równania ruchu ciepła w obiekcie podczas procesu walcowania gwintów przy wykorzystaniu metod jawnego i niejawnego całkowania. Zamieszczono przykładowe wyniki analiz numerycznych dla procesu walcowania gwintów w programie ANSYS. Pokazano również rozkłady temperatur dla różnych wartości prędkości walcowania.

Abstract

In the this paper the solutions of discrete equations of the heat transfer of the object in the thread rolling process with applied explicit and implicit integrations methods, were shown. Examples of simulations of the rolling process in ANSYS programs are presented. Also the temperature distributions for various value of rolling velocity were shown.

Słowa kluczowe:
walcowanie gwintów, eko-modelowanie, ekologiczne procesy technologiczne, sformułowanie wariacyjne, metoda elementów skończonych

Keywords:
thread rolling, eco-modelling, ecological technological process, variational formulation, Finite Element Method